

1 **High-quality reference genome for an arid-adapted mammal, the banner-tailed kangaroo**  
2 **rat (*Dipodomys spectabilis*)**

3 Avril M. Harder<sup>1\*</sup>, Kimberly K.O. Walden<sup>2</sup>, Nicholas J. Marra<sup>3</sup>, Janna R. Willoughby<sup>1</sup>

4 1. School of Forestry and Wildlife Sciences, Auburn University, Auburn, Alabama, USA

5 2. Roy J. Carver Biotechnology Center, University of Illinois at Urbana-Champaign, Urbana,  
6 Illinois, USA

7 3. Division of Science, Mathematics, and Technology, Governors State University, University  
8 Park, Illinois, USA

9 \*Author for correspondence: Avril Harder, School of Forestry and Wildlife Sciences, Auburn  
10 University, Auburn, Alabama, USA, (773) 688-8564, [avrilharder@gmail.com](mailto:avrilharder@gmail.com)

11 **Abstract**

12 Kangaroo rats in the genus *Dipodomys* are found in a variety of habitat types in western North  
13 America, including deserts, arid and semi-arid grasslands, and scrublands. Many *Dipodomys*  
14 species are experiencing strong population declines due to increasing habitat fragmentation, with  
15 two species listed as federally endangered. The precarious state of many *Dipodomys* populations,  
16 including those occupying extreme environments, make species of this genus valuable subjects  
17 for studying the impacts of habitat degradation and fragmentation on population genomic  
18 patterns and for characterizing the genomic bases of adaptation to harsh conditions. To facilitate  
19 exploration of such questions, we assembled and annotated a reference genome for the banner-  
20 tailed kangaroo rat (*D. spectabilis*) using PacBio HiFi sequencing reads, providing a more  
21 contiguous genomic resource than two previously assembled *Dipodomys* genomes. Using the  
22 HiFi data for *D. spectabilis* and publicly available sequencing data for two other *Dipodomys*  
23 species (*D. ordii* and *D. stephensi*), we demonstrate the utility of this new assembly for studies of  
24 congeners by conducting inference of historic effective population sizes ( $N_e$ ) and linking these  
25 patterns to the species' current extinction risk statuses. The genome assembly presented here will  
26 serve as a valuable resource for population and conservation genomic studies of *Dipodomys*  
27 species, comparative genomic research within mammals and rodents, and investigations into  
28 genomic adaptation to extreme environments and changing landscapes.

29 **Key words**

30 mammal genomics, Pacific Biosciences, demographic history

## 31 **Significance statement**

32 Kangaroo rats in the genus *Dipodomys* occur in a wide variety of habitat types, ranging from  
33 scrublands to arid deserts, and are increasingly impacted by habitat fragmentation with  
34 populations of many species in strong decline. To facilitate population and conservation genomic  
35 studies of *Dipodomys* species, we generated the first reference genome assembly for the  
36 extensively studied banner-tailed kangaroo rat (*D. spectabilis*) from long read PacBio sequencing  
37 data. The genome assembly presented here will serve as a valuable resource for studies of  
38 *Dipodomys* species—which have long served as ecological and physiological models for the  
39 study of osmoregulation—comparative genomic surveys of mammals and rodents, and  
40 investigations into genomic adaptation to extreme environments and changing landscapes.

## 41 **Introduction**

42 The genus *Dipodomys* comprises 20 species of kangaroo rats and belongs to the Heteromyidae  
43 family of rodents (Alexander & Riddle 2005). Often considered keystone species, kangaroo rats  
44 inhabit warm and cold deserts, arid and semi-arid grasslands, and scrublands of western North  
45 America, with most species preferring sandy soils that allow for construction of elaborate  
46 underground burrows used for protection from predators and harsh environmental conditions,  
47 reproduction, and food caching (Alexander & Riddle 2005; Brown & Heske 1990). For many of  
48 these species, limited dispersal capabilities and habitat fragmentation has led to population  
49 declines, with five species classified as threatened by IUCN (International Union for  
50 Conservation of Nature) and two species (and four additional subspecies) listed as federally  
51 endangered, of which several have been the subject of management efforts to decrease species  
52 vulnerability (IUCN 2021; Shier et al. 2021; Hendricks et al. 2020; Blackhawk et al. 2016; Loew

53 et al. 2006). The imperiled state of many *Dipodomys* populations, combined with the vast array  
54 of occupied habitat types that include arid environments, make species of this genus valuable  
55 subjects for studying the impacts of habitat degradation and fragmentation on population  
56 genomic patterns and for characterizing the genomic bases of adaptation to extreme  
57 environments. Specifically, the latter application may provide a key link between historical  
58 studies of *Dipodomys* kidney morphology (Vimtrup & Schmidt-Nielsen 1952; Schmidt-Nielsen  
59 & Schmidt-Nielsen 1952) and more recent investigations of gene and protein expression related  
60 to osmoregulation in arid conditions (reviewed in Rocha et al. 2021).

61 To facilitate genomic studies of *Dipodomys* species, we used PacBio HiFi sequencing  
62 data to generate an annotated reference genome for the banner-tailed kangaroo rat (*D.*  
63 *spectabilis*), a species whose ecology and evolution has been studied extensively for several  
64 decades (Vorhies & Taylor 1922; Greene & Reynard 1932; Schroder 1979; Waser & Jones 1991;  
65 Busch et al. 2007; Willoughby et al. 2019). Prior to the assembly of this genome, two *Dipodomys*  
66 reference genomes were available that had been built with short read sequencing data, with one  
67 assembly comprising 1.3 million scaffolds totaling 2.3 Gb (*D. stephensi*, GCA\_004024685.1)  
68 and the other comprising 65,193 scaffolds totaling 2.2 Gb (*D. ordii*, GCA\_000151885.2). We  
69 used long read sequencing data to generate a *D. spectabilis* assembly with increased contiguity  
70 and then used short read sequences from *D. ordii* and *D. stephensi* to conduct historical effective  
71 population size ( $N_e$ ) inference for all three species. We compared population trajectories for  
72 these two species and *D. spectabilis* to identify demographic trends associated with current  
73 extinction risk designations of the species, which range from IUCN listings of least concern (*D.*  
74 *ordii*) and near threatened (*D. spectabilis*) to vulnerable and U.S. federally endangered (*D.*

75 *stephensi*). These analyses highlight the utility of the *D. spectabilis* reference genome for  
76 exploring evolutionary questions with conservation implications.

## 77 **Results and Discussion**

### 78 *Genome assembly and annotation*

79 We generated 97.9 Gb of PacBio HiFi reads resulting in 23X coverage of the final assembly. The  
80 hifiasm primary contig assembly summed to 2.8 Gb and comprised 2,026 contigs with an  
81 assembly contig N50 of 9.6 Mb (Table 1). Prior to annotation, Benchmarking Universal Single-  
82 Copy Orthologs (BUSCO) v5.1.2 assessment identified 97.2% of vertebrata\_odb10 orthologs as  
83 complete (94.2% single-copy, 3.0% duplicated), 1.1% as fragmented, and 1.7% as missing.  
84 Identification of repetitive sequences with WindowMasker resulted in the masking of 47.85% of  
85 the genome sequence. Annotation of the masked genome via NCBI's pipeline identified 20,632  
86 protein-coding genes with a mean of 1.66 transcripts per gene and an average gene length of  
87 31,775 bp. The BUSCO v4.1.4 results for the annotated gene set classified 98.2% of  
88 glires\_odb10 orthologs as complete (96.5% single-copy, 1.7% duplicated), 0.4% as fragmented,  
89 and 1.5% as missing.

90 Prior to assembly of the *D. spectabilis* genome, the most contiguous *Dipodomys*  
91 reference genome was built for *D. ordii* (GCA\_000151885.2). The *D. spectabilis* assembly is  
92 nearly 800 Mb larger than the ungapped *D. ordii* assembly with a markedly improved contig N50  
93 (9.6 Mb) over *D. ordii* (48,087 bp) and is organized into far fewer sequences (2,026 contigs) than  
94 the *D. ordii* assembly (148,226 contigs organized into 65,193 scaffolds). Furthermore, the  
95 longest contigs in the *D. spectabilis* assembly (maximum = 60.9 Mb) approach lengths typical of

96 mammalian chromosome arms (Klegarth & Eisenberg 2018). The new *D. spectabilis* annotation  
97 also comprises a greater number of fully-supported mRNA sequences than the *D. ordii* assembly  
98 (33,775 vs. 22,964) and will provide increased resolution to genomic studies of *Dipodomys* that  
99 aim to describe patterns of adaptation and signals of selection.

100 **Table 1.** Genome assembly and annotation statistics for *Dipodomys spectabilis*.

Elements	Current version
Genome assembly	
Assembly size (Mb)	2,845
Number of contigs	2,026
Longest contig (Mb)	60.9
N50 contig length (Mb)	9.6
GC (%)	40.8
Gaps (%)	0
BUSCO completeness (%)	97.2
Gene annotation	
Protein-coding genes	20,632
Mean transcripts per gene	1.66
Mean gene length (bp)	31,775
Mean exons per transcript	10.32
Mean exon length (bp)	243
Mean intron length (bp)	4,673
BUSCO completeness (%)	98.2

101 *Variant calling*

102 For both *D. ordii* and *D. stephensi*, read mapping rates to the *D. spectabilis* reference genome  
103 were high (95.9% and 92.1%, respectively), demonstrating the utility of this assembly for  
104 genomic studies across the genus despite the approximately 10 million years separating these  
105 three species from their most recent common ancestor (Figure 1A). After the final filtering step  
106 for PSMC (*i.e.*, retaining sites with read depths greater than 1/3 and less than two times the

107 average depth of coverage within a sample), we retained genotypes for a total of 2.3 billion sites  
108 for *D. spectabilis*, 1.7 billion for *D. stephensi*, and 1.7 billion for *D. ordii*. The proportion of  
109 heterozygous sites was lowest for *D. ordii* (0.0012) and was similar between *D. spectabilis*  
110 (0.0021) and *D. stephensi* (0.0023). Mapping to a congeneric reference genome could result in  
111 biased estimates of heterozygosity. Because *D. ordii* and *D. stephensi* are more closely related to  
112 one another than either species is to *D. spectabilis* (Figure 1A), mapping bias is expected to  
113 affect estimates for *D. ordii* and *D. stephensi* in the same direction (i.e., either under- or  
114 overestimation) and with similar magnitude. However, our heterozygosity results are not  
115 consistent with such a pattern. For *D. ordii*, the heterozygosity result contrasts with the much  
116 larger range documented for *D. ordii* than for the other two species (Figure 1B), but the low  
117 heterozygosity of the *D. ordii* sample likely reflects the recent demographic history of the  
118 sequenced individual's population of origin, rather than long-term, species-level trends.

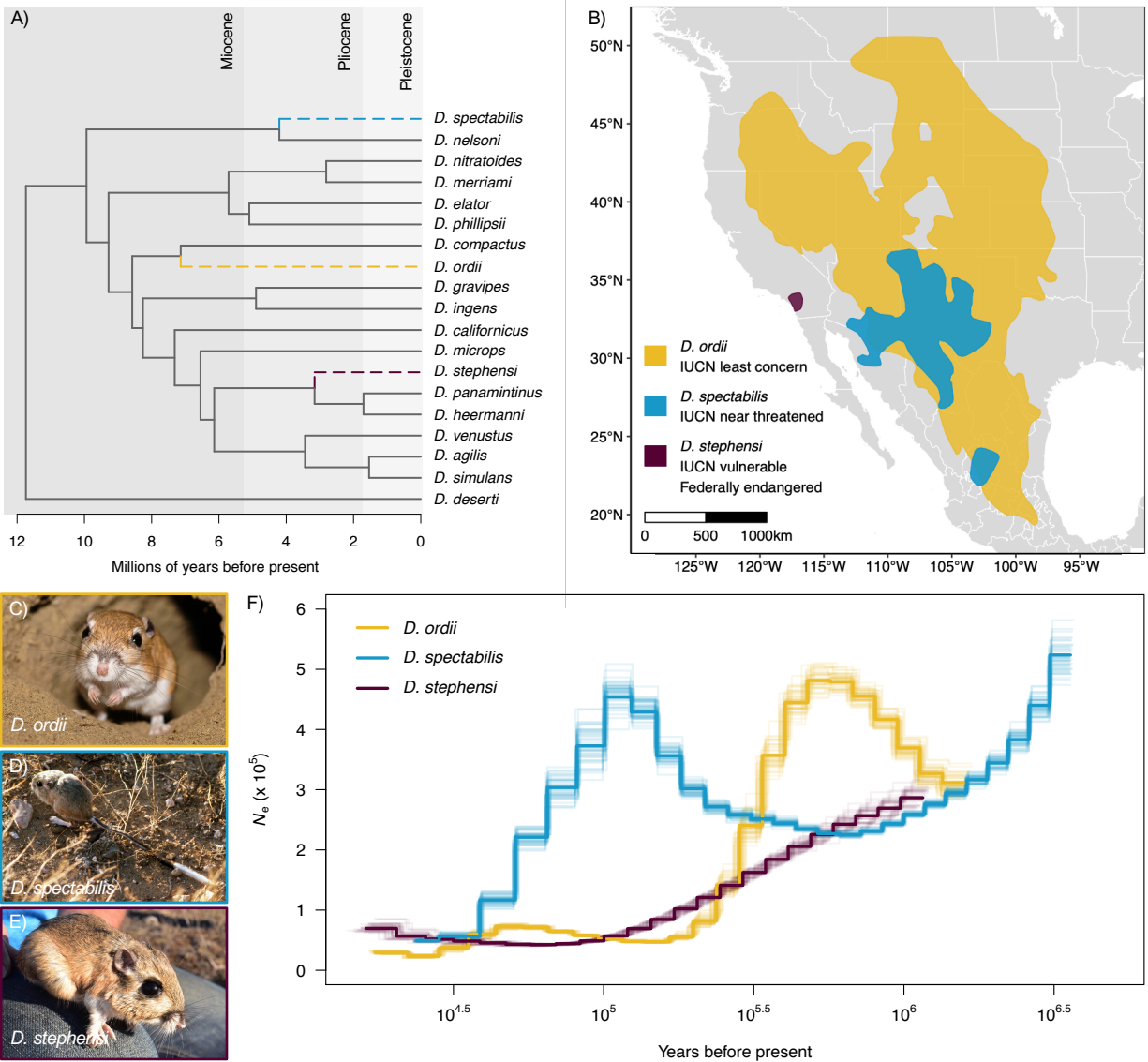
### 119 *Historical effective population size inference*

120 Each of the three species we analyzed displays distinct patterns of historical  $N_e$  as inferred from  
121 PSMC analysis (Figure 1F). *D. ordii* and *D. spectabilis* both exhibit peaks in historical  $N_e$   
122 followed by declines, whereas *D. stephensi* appears to have experienced steadily declining  $N_e$   
123 over the time range covered by our analysis. The range of time over which changes in  $N_e$  were  
124 inferred for *D. spectabilis* extends approximately 2 million years farther into the past than the  
125 time ranges for *D. ordii* and *D. stephensi*. The increased temporal range of PSMC results for *D.*  
126 *spectabilis* relative to the other two species is likely due to the use of long-read data to identify  
127 variants, which allows for resolution of longer haplotypes and, consequently, inference of older  
128 coalescent events compared to when variants are called from short-read data.

129           Initially, diversification within heteromyid rodents likely took place towards the middle  
130 of the Miocene (Figure 1A), around the time that habitat types were also diversifying across their  
131 western North America ranges. Further speciation within *Dipodomys* coincided with continuing  
132 partitioning of ecoregions and cyclical formation of glacial refugia into the Pleistocene  
133 (Alexander & Riddle 2005). Although all three species exhibit declines in historical  $N_e$ , the  
134 steady decline observed for *D. stephensi* is consistent with this species' extremely limited current  
135 range and U.S. federally endangered status. Both *D. spectabilis* and *D. ordii* maintain much  
136 larger contemporary range sizes than *D. stephensi* and are of relatively less conservation  
137 concern. Declines in  $N_e$  for these species may correspond to disrupted movement patterns among  
138 populations during Pleistocene glacial-interglacial cycles.

139           Through these analyses, we have demonstrated the applicability of our new *D. spectabilis*  
140 reference genome to genomic studies across the genus *Dipodomys*, a taxon comprising species  
141 with a broad range of conservation statuses and habitat preferences. Our annotated assembly  
142 represents a significant improvement in resources for this genus and will facilitate future  
143 investigations into a broad range of eco-evolutionary questions, including for species of  
144 conservation concern, such as *D. stephensi*, or for other *Dipodomys* species experiencing  
145 increasing habitat fragmentation and population declines (Blackhawk et al. 2016; Hendricks et  
146 al. 2020).





147 **Figure 1.** A) *Dipodomys* phylogeny constructed using the TimeTree database. The most recent  
 148 common ancestor of *D. spectabilis*, *D. ordii*, and *D. stephensi* lived approximately 10 million  
 149 years ago. B) Current ranges and conservation statuses for *D. ordii*, *D. spectabilis*, and *D.*  
 150 *stephensi* in western North America. C-E) Photos of *D. ordii*, *D. spectabilis*, and *D. stephensi*. F)  
 151 PSMC results for all three species, plotted using a generation time of 1 year and a substitution  
 152 rate of  $2.2e-9$  per base pair per year. Lighter lines represent results of 50 bootstrap replicates per  
 153 species. Map made with Natural Earth and the *rnaturalearth* package in R using the WGS84  
 154 coordinate system. Species range shapefiles downloaded from IUCN (IUCN 2008, 2009, 2018).  
 155 Image credits: Andy Teucher (*D. ordii*; <https://bit.ly/3Cpcjfl>), Peter Waser (*D. spectabilis*),  
 156 USFWS Pacific Southwest Region (*D. stephensi*; <https://bit.ly/3nsHPVu>).

## 157 **Materials and Methods**

### 158 *Sample collection and sequencing*

159 The male *Dipodomys spectabilis* individual used for genomic sequencing was collected near  
160 Portal, AZ (31°56'N, 109°5'W) in December 2009. Whole organs (kidney and liver) were  
161 dissected and frozen in liquid nitrogen for transport to Purdue University and subsequent storage  
162 at -80 °C (Marra et al. 2014, 2012). In February 2021, 0.1 g portions of both tissues were shipped  
163 on dry ice to Polar Genomics (Ithaca, NY) for extraction of high-molecular weight genomic  
164 DNA (gDNA) using a modified nuclei extraction protocol (Zhang et al. 2012). Extracted gDNA  
165 was supplied to the Roy J. Carver Biotechnology Center DNA services core (University of  
166 Illinois) where it was sheared to an average fragment length of 13kb with a Megaruptor 3.  
167 Sheared gDNA was converted to a PacBio library with the SMRTBell Express Template Prep  
168 Kit 2.0, and this library was sequenced on 6 SMRT cells 8M on a PacBio Sequel Iie using the  
169 circular consensus sequencing (CCS) mode and a 30-hour movie time to produce HiFi reads.  
170 CCS analysis was performed using SMRTLink V10.0 using default parameters.

### 171 *Genome assembly and annotation*

172 PacBio HiFi reads were filtered to retain those between 4 kb and 40 kb with seqkit (Shen et al.  
173 2016) and then assembled with hifiasm v.0.14.2 (r315) using default parameters (Cheng et al.  
174 2021). Genome completeness was assessed using BUSCO v.5.1.2 in “genome” mode with the  
175 vertebrata\_odb10 lineage dataset (3,354 orthologs) (Manni et al. 2021).

176 Annotation of genes and genomic features from the hifiasm primary contigs was  
177 conducted by NCBI via the Eukaryotic Genome Annotation Pipeline v9.0 (release date June 8  
178 2021) (Thibaud-Nissen et al. 2013). This pipeline includes repeat masking using WindowMasker  
179 (Morgulis et al. 2006) and gene model prediction for the masked genome informed by NCBI

180 RefSeq transcript and protein sets for *Mus musculus* and publicly available RNA-Seq data. The  
181 RNA-Seq reads used for gene prediction originated from kidney and spleen tissues of *D.*  
182 *spectabilis* and two other heteromyid rodents (*Heteromys desmarestianus* and *Chaetodipus*  
183 *baileyi*). The details of the NCBI annotation pipeline can be found at:  
184 [https://www.ncbi.nlm.nih.gov/genome/annotation\\_euk/process/](https://www.ncbi.nlm.nih.gov/genome/annotation_euk/process/). The final annotation (NCBI  
185 *Dipodomys spectabilis* Annotation Release 100) was assessed using BUSCO v4.1.4 in “protein”  
186 mode using the glires\_odb10 lineage data set (13,798 orthologs) (Simão et al. 2015).

### 187 *Variant calling*

188 We downloaded Illumina sequencing reads from NCBI’s Sequence Read Archive (SRA) that  
189 were previously used in assembly of the *D. ordii* and *D. stephensi* reference genomes (*D. ordii*  
190 sequence accessions SRR1646412-23 and *D. stephensi* sequence accession SRR14572526). We  
191 removed adapter sequences and clipped low quality bases (quality score < 20) from both ends of  
192 reads using Trimmomatic v0.39 (Bolger et al. 2014). Reads were quality-checked before and  
193 after trimming using FastQC v0.11.9 (Andrews 2015) and were aligned to the newly assembled  
194 *D. spectabilis* reference genome using the BWA-MEM algorithm implemented in BWA v0.7.12  
195 (Li 2013). To align our HiFi reads for the *D. spectabilis* individual to the assembled genome, we  
196 used the map-hifi option in Minimap2 (Li 2018). When necessary, we merged resulting BAM  
197 files into a single file per species using SAMtools v1.11 (Li et al. 2009). Finally, we sorted the  
198 BAM files and calculated average depth of coverage across each contig, again using SAMtools.

199 For each species, a variant file was produced using the BCFtools v1.10.2 mpileup and  
200 call commands (Danecek et al. 2021). We initially filtered each VCF file to exclude indels (*i.e.*,  
201 retain SNPs) and to retain only sites with quality scores > 30 and minimum read depth of 15  
202 using VCFtools v0.1.14 (Danecek et al. 2011). Variants were further limited to those located on

203 contigs  $\geq$  100 kb in length and contigs likely not originating from sex chromosomes, leaving  
204 variants on 652 contigs totaling 2.55 Gb in length (89.7% of reference assembly).

### 205 *Inference of historical effective population sizes*

206 To compare patterns of historical effective population size ( $N_e$ ) among *Dipodomys* species, we  
207 began by using the BCFtools vcfutils.pl script and the PSMC fq2psmcfa function (Li & Durbin  
208 2011) to convert the VCF files to masked consensus FASTA files. For each file, we applied a  
209 final variant filter to exclude sites with read depths less than 1/3 and greater than two times the  
210 average depth of coverage calculated for each sample above, as recommended by the PSMC  
211 authors (<https://github.com/lh3/psmc>), and determined the proportion of heterozygous sites.  
212 After first testing default PSMC parameter settings, we ultimately set the -p parameter to  
213 '8+25\*2+2+4' and confirmed that at least ten recombination events were inferred in each  
214 interval within 20 iterations before also performing 50 iterations of bootstrapping. We plotted the  
215 results in R v4.0.3 (R Core Team 2020), supplying the average mammalian mutation rate (2.2e-9  
216 per base pair per year) (Kumar & Subramanian 2002) and a generation time of 1 year to the  
217 functions defined in the plotPsmc.R script published on Dryad (Liu & Hansen 2017, 2016). To  
218 place the PSMC results into broader taxonomic context, we also constructed a *Dipodomys*  
219 phylogeny using a Newick file exported from the TimeTree database (Kumar et al. 2017) and  
220 plotted using the *ape* package in R.

### 221 **Data Availability**

222 Genome assembly and raw sequencing data have been deposited at the NCBI under the  
223 accessions GCA\_019054845.1 and SRX11001182-SRX11001186, respectively. Genome

224 annotation is available under the NCBI accession ASM1905484v1. Code for all bioinformatic  
225 analyses available at [https://github.com/avril-m-harder/D\\_spectabilis\\_genome\\_resource](https://github.com/avril-m-harder/D_spectabilis_genome_resource) and  
226 [https://github.com/jwillou/D\\_spectabilis\\_genome\\_resource](https://github.com/jwillou/D_spectabilis_genome_resource).

## 227 **Acknowledgements**

228 This material is based on work supported by the National Science Foundation Postdoctoral  
229 Research Fellowships in Biology Program under Grant No. 2010251 to AMH. This work was  
230 also supported by the U.S. Department of Agriculture, National Institute of Food and  
231 Agriculture, Hatch project 1025651 to JRW. We thank J. Vrebalov of Polar Genomics for  
232 performing DNA extraction and the University of Illinois' Roy J. Carver Biotechnology Center  
233 DNA Services Lab for library construction and sequencing.

## 234 Literature Cited

- 235 Alexander LF, Riddle BR. 2005. Phylogenetics of the New World rodent family Heteromyidae.  
236 *Journal of Mammalogy*. 86:366–379. doi: 10.1644/BER-120.1.
- 237 Andrews S. 2015. *FastQC: A quality control tool for high throughput sequence data*.  
238 <http://www.bioinformatics.babraham.ac.uk/projects/fastqc/>.
- 239 Blackhawk NC, Germano DJ, Smith PT. 2016. Genetic variation among populations of the  
240 endangered giant kangaroo rat, *Dipodomys ingens*, in the southern San Joaquin Valley. *The*  
241 *American Midland Naturalist*. 175:261–274. doi: 10.1674/0003-0031-175.2.261.
- 242 Bolger AM, Lohse M, Usadel B. 2014. Trimmomatic: a flexible trimmer for Illumina sequence  
243 data. *Bioinformatics*. 30:2114–2120. doi: 10.1093/bioinformatics/btu170.
- 244 Brown JH, Heske EJ. 1990. Control of a desert-grassland transition by a keystone rodent guild.  
245 *Science*. 250:1705–1707. doi: 10.1126/science.250.4988.1705.
- 246 Busch JD, Waser PM, DeWoody JA. 2007. Recent demographic bottlenecks are not  
247 accompanied by a genetic signature in banner-tailed kangaroo rats (*Dipodomys spectabilis*).  
248 *Molecular Ecology*. 16:2450–2462.
- 249 Cheng H, Concepcion GT, Feng X, Zhang H, Li H. 2021. Haplotype-resolved de novo assembly  
250 using phased assembly graphs with hifiasm. *Nature Methods*. 18:170–175.
- 251 Danecek P et al. 2011. The variant call format and VCFtools. *Bioinformatics*. 27:2156–2158.  
252 doi: 10.1093/bioinformatics/btr330.
- 253 Danecek P et al. 2021. Twelve years of SAMtools and BCFtools. *GigaScience*. 10:giab008. doi:  
254 10.1093/gigascience/giab008.
- 255 Greene RA, Reynard C. 1932. The influence of two burrowing rodents, *Dipodomys spectabilis*  
256 *spectabilis* (kangaroo rat) and *Neotoma albigula albigula* (pack rat) on desert soils in Arizona.  
257 *Ecology*. 13:73–80. doi: 10.2307/1932493.
- 258 Hendricks S et al. 2020. Patterns of genetic partitioning and gene flow in the endangered San  
259 Bernardino kangaroo rat (*Dipodomys merriami parvus*) and implications for conservation  
260 management. *Conservation Genetics*. 21:819–833. doi: 10.1007/s10592-020-01289-z.
- 261 IUCN 2008. *Dipodomys ordii*. The IUCN Red List of Threatened Species. Version 2021-2
- 262 IUCN SSC Small Mammal Specialist Group 2018. *Dipodomys stephensi*. The IUCN Red List of  
263 Threatened Species. Version 2021-2
- 264 IUCN SSC Small Mammal Specialist Group 2019. *Dipodomys spectabilis*. The IUCN Red List  
265 of Threatened Species. Version 2021-2

- 266 IUCN 2021. *The IUCN Red List of Threatened Species*. <https://www.iucnredlist.org> (Accessed  
267 November 1, 2021).
- 268 Klegarth AR, Eisenberg DTA. 2018. Mammalian chromosome–telomere length dynamics. *Royal  
269 Society Open Science*. 5:180492. doi: 10.1098/rsos.180492.
- 270 Kumar S, Stecher G, Suleski M, Hedges SB. 2017. TimeTree: A resource for timelines,  
271 timetrees, and divergence times. *Molecular Biology and Evolution*. 34:1812–1819. doi:  
272 10.1093/molbev/msx116.
- 273 Kumar S, Subramanian S. 2002. Mutation rates in mammalian genomes. *Proceedings of the  
274 National Academy of Sciences*. 99:803–808. doi: 10.1073/pnas.022629899.
- 275 Li H. 2013. Aligning sequence reads, clone sequences and assembly contigs with BWA-MEM.  
276 arXiv:1303.3997 [q-bio]. <http://arxiv.org/abs/1303.3997> (Accessed May 8, 2017).
- 277 Li H. 2018. Minimap2: pairwise alignment for nucleotide sequences. *Bioinformatics*. 34:3094–  
278 3100. doi: 10.1093/bioinformatics/bty191.
- 279 Li H et al. 2009. The sequence alignment/map format and SAMtools. *Bioinformatics*. 25:2078–  
280 2079. doi: 10.1093/bioinformatics/btp352.
- 281 Li H, Durbin R. 2011. Inference of human population history from individual whole-genome  
282 sequences. *Nature*. 475:493–496. doi: 10.1038/nature10231.
- 283 [dataset]\* Liu S, Hansen MM. 2016. Data from: PSMC (pairwise sequentially Markovian  
284 coalescent) analysis of RAD (restriction site associated DNA) sequencing data. *Dryad. Dataset*.  
285 doi: <https://doi.org/10.5061/dryad.0618v>.
- 286 Liu S, Hansen MM. 2017. PSMC (pairwise sequentially Markovian coalescent) analysis of RAD  
287 (restriction site associated DNA) sequencing data. *Molecular Ecology Resources*. 17:631–641.  
288 doi: 10.1111/1755-0998.12606.
- 289 Loew SS, Williams DF, Ralls K, Pilgrim K, Fleischer RC. 2006. Population structure and genetic  
290 variation in the endangered Giant Kangaroo Rat (*Dipodomys ingens*). *Conservation Genetics*.  
291 6:495–510. doi: 10.1007/s10592-005-9005-9.
- 292 Manni M, Berkeley MR, Seppely M, Simão FA, Zdobnov EM. 2021. BUSCO update: novel and  
293 streamlined workflows along with broader and deeper phylogenetic coverage for scoring of  
294 eukaryotic, prokaryotic, and viral genomes. arXiv. 2106.11799.
- 295 Marra NJ, Eo SH, Hale MC, Waser PM, DeWoody JA. 2012. *A priori* and *a posteriori*  
296 approaches for finding genes of evolutionary interest in non-model species: Osmoregulatory  
297 genes in the kidney transcriptome of the desert rodent *Dipodomys spectabilis* (banner-tailed  
298 kangaroo rat). *Comparative Biochemistry and Physiology Part D: Genomics and Proteomics*.  
299 7:328–339. doi: 10.1016/j.cbd.2012.07.001.

- 300 Marra NJ, Romero A, DeWoody JA. 2014. Natural selection and the genetic basis of  
301 osmoregulation in heteromyid rodents as revealed by RNA-seq. *Molecular Ecology*. 23:2699–  
302 2711. doi: 10.1111/mec.12764.
- 303 Morgulis A, Gertz EM, Schaffer AA, Agarwala R. 2006. WindowMasker: window-based masker  
304 for sequenced genomes. *Bioinformatics*. 22:134–141. doi: 10.1093/bioinformatics/bti774.
- 305 R Core Team. 2020. *R: a language and environment for statistical computing*. R Foundation for  
306 Statistical Computing: Vienna, Austria <https://www.R-project.org/>.
- 307 Rocha JL, Godinho R, Brito JC, Nielsen R. 2021. Life in deserts: The genetic basis of  
308 mammalian desert adaptation. *Trends in Ecology & Evolution*. 36:637–650. doi:  
309 10.1016/j.tree.2021.03.007.
- 310 Schmidt-Nielsen K, Schmidt-Nielsen B. 1952. Water metabolism of desert mammals.  
311 *Physiological Reviews*. 32:135–166. doi: 10.1152/physrev.1952.32.2.135.
- 312 Schroder GD. 1979. Foraging behavior and home range utilization of the bannertail kangaroo rat  
313 (*Dipodomys spectabilis*). *Ecology*. 60:657–665. doi: 10.2307/1936601.
- 314 Shen W, Le S, Li Y, Hu F. 2016. SeqKit: A cross-platform and ultrafast toolkit for FASTA/Q  
315 file manipulation. *PLoS ONE*. 11:e0163962. doi: 10.1371/journal.pone.0163962.
- 316 Shier DM et al. 2021. Genetic and ecological evidence of long-term translocation success of the  
317 federally endangered Stephens' kangaroo rat. *Conservation Science and Practice*. 3. doi:  
318 10.1111/csp2.478.
- 319 Simão FA, Waterhouse RM, Ioannidis P, Kriventseva EV, Zdobnov EM. 2015. BUSCO:  
320 assessing genome assembly and annotation completeness with single-copy orthologs.  
321 *Bioinformatics*. 31:3210–3212. doi: 10.1093/bioinformatics/btv351.
- 322 Thibaud-Nissen F, Souvorov A, Murphy T, DiCuccio M, Kitts P. 2013. Eukaryotic Genome  
323 Annotation Pipeline. In: *The NCBI Handbook* [Internet]. Bethesda (MD): National Center for  
324 Biotechnology Information.
- 325 Vimtrup BJ, Schmidt-Nielsen B. 1952. The histology of the kidney of kangaroo rats. *The*  
326 *Anatomical Record* 114:515–528. doi: 10.1002/ar.1091140402.
- 327 Vorhies CT, Taylor WP. 1922. Life history of the kangaroo rat, *Dipodomys spectabilis*  
328 *spectabilis* Merriam. U.S. Department of Agriculture Bulletin. 1901:1–40.
- 329 Waser PM, Jones WT. 1991. Survival and reproductive effort in banner-tailed kangaroo rats.  
330 *Ecology*. 72:771–777. doi: 10.2307/1940579.
- 331 Willoughby JR, Waser PM, Brüniche-Olsen A, Christie MR. 2019. Inbreeding load and  
332 inbreeding depression estimated from lifetime reproductive success in a small, dispersal-limited  
333 population. *Heredity*. 123:192–201. doi: 10.1038/s41437-019-0197-z.



334 Zhang M et al. 2012. Preparation of megabase-sized DNA from a variety of organisms using the  
335 nuclei method for advanced genomics research. *Nature Protocols*. 7:467–478. doi:  
336 10.1038/nprot.2011.455.